CALIBRATING THE QUIKSCAT/SEAWINDS RADAR FOR MEASURING RAINRATE OVER THE OCEANS

David E. Weissman
Dept. of Engineering
Hofstra University, Hempstead, New York 11549
Tel:(516) 463-5546; Fax: (516) 463-4939
E-Mail: eggdew@hofstra.edu

Mark A. Bourassa
COAPS/The Florida State University, Tallahassee, FL 32306-2840

Jeffrey Tongue
National Weather Service, Upton, New York 11973

Abstract

This effort continues a study of the effects of rain, over the oceans, on the signal retrieved by the SeaWinds scatterometer. It is determined that the backscatter radar cross section can be used to estimate the volumetric rain rate, averaged horizontally, across the surface resolution cells of the scatterometer. The dual polarization of the radar has a key role in developing this capability. The relative magnitudes of the radar backscatter depends on the volumetric rainrate, the rain column height and surface wind velocity, the viewing angle, as well as the polarization (due to the oblateness of raindrops at the higher rainrates). The approach to calibrating the SeaWinds normalized radar cross section (NRCS) is to collect NWS NEXRAD radar-derived rainrate measurements (4 km spatial resolution and 6 minute rotating cycles) co-located in space (offshore) and time with scatterometer observations. These calibration functions lead to a Z-R relationship, which is then used at mid-ocean locations to estimate the rainrate in 0.25° or larger resolution cells, which are compared with TRMM TMI rain estimates. Experimental results to date are in general agreement with simplified theoretical models of backscatter from rain, for this frequency, 14 GHz. These comparisons show very good agreement on a cell-by-cell basis with the TMI estimates for both wide areas (1000 KM) and smaller area rain events.

Manuscript submitted for publication to IEEE Transactions on Geoscience and Remote Sensing
September 2002

I. INTRODUCTION

Rain interferes with the intended application of the measurements of the sea surface's radar cross section by the SeaWinds scatterometer: the estimation of the sea surface wind speed and direction [1],[2]. The presence of rain regions within the boundaries of the illuminated surface area results in additional backscatter from these atmospheric volumes, and possibly attenuation of the beam directed towards the surface and the backscatter from the surface. In many cases, depending on the wind magnitude, the backscatter from the rain will augment or dominate the received signal and the measured NRCS. This results in overestimates of the wind magnitude, and meaningless wind direction values [3]. The relatively long duration transmitted pulse provides the equivalent of a continuous-wave radar. The backscatter from the rain volume is the path-integrated value that may include the complete column of rain, or possibly a thinner layer when the beam attenuation is large enough to suppress most of the power density before it reaches the sea surface.

Steps were taken to quantify the effect of rain on SeaWinds NRCS, using NEXRAD Level III rain data for in-situ measurements, over the ocean and sufficiently far offshore to avoid land contamination issues. The near simultaneous NEXRAD composite reflectivity data ("Z" values; e.g., Figure 1), were converted to rainrate in 4 km cells, then they were combined into an average over an approximate scatterometer footprint (a 28 km square), centered at each scatterometer cell. Each of the co-located SeaWinds NRCS's, subset by polarization, are assigned to that average rainrate. The wide variation of the rain intensity within the area spanned by the scatterometer swath results in a sizeable dynamic range of NRCS values. These data provide the basis of calibration curves for each polarization; these curves are referred to as Z-R functions in radar meteorology terminology. These functions are used over the open ocean to convert the QSCAT L2A NRCS data into rainrate estimates. The rain estimates can then be compared with values derived from the passive microwave imager (TMI) onboard the TRMM satellite. Numerous events in disparate ocean regions were analyzed and all produced consistently good agreement between the TMI and this SeaWinds-algorithm rainrate for averages over a 0.5° square latitude/longitude region.

II. BACKGROUND

A co the al cy al ch the req an
Th meas of oc bee or
goal or to ffec te an th osph Th ar im
ap to pred an al im m req
ter Th T op cal R al Measu M (TRMM a 99 du
ts rop cal fal araph tatements ad abo
TRMM rad Ku al [-]. te es the di tri
op cal p despe eeded an ifi ice al odel of
obal On TRMM trumen ad [ ]. Th featu
mpared to tech th abi ty pen te se to the
th return gnal de profi the rat gh pa ol

Rai f the m di sp ables its oge
to cl an to pa al and p poral
hen soph ted eather radars perf eas m at f im ati estimati
th se parame gene ff an to ou of
elated th umi the of op N erth th se ad
pr bee ac ted as th be od
50 The de elopm of QSCAT ecl be fi m large bod
ed th fi teorol on fo gr
mm of se ors to tellite rad bri an pe od rv ac loc
ad ances th pat al erag bu es gn ant eeds. The W ad th
de th. mak bstantial tribu to be sp ial an poral erag
bec ar spaceborn rad be TRMM A
tril th L itat of ad
he ted tp an ack of fre po al pl too to te
nd an be ed W ids
nc to th 400 th H- an ol obser ati
depend ice

capabilities.

One recent innovation gaining increased application is coherent dual-polarization backscatter measurements to discriminate between the smaller spherical raindrops and the larger oblate drops, the distributions of which are functions of rainrate. The difference of H-pol and V-pol signals due to this effect is called "differential-reflectivity"[6]. While SeaWinds is limited to incoherent dual-polarization, it still has the capability to exploit this phenomenon. This differential polarization response of the SeaWinds scatterometer to moderate and large rainrates can be exploited for quantitative precipitation detection and measurement on many different time and spatial scales. This technique has been applied across a wide of frequencies from 3 to 35 Ghz [7]. Of particular relevance to SeaWinds, is that Holt [7] shows that the key measurable parameter, the differential reflectivity (Z_{DR}), has a very similar dependence on dropsize and rainrate at 16 GHz (Ku-band) as it does at 3 GHz (S-Band) which is the nominal National Weather Service NEXRAD radars' frequency.

III. APPROACH

The virtually instantaneous co-location of NEXRAD rain measurements with QuikSCAT and buoy observations is an advance in the quantitative determination of the effect of rainfall on QuikSCAT NRCS data. The NEXRAD data products consist of radar scans taken only 6 minutes apart, so that the time coincidences with QSCAT observations are sufficiently close to be viewed as effectively instantaneous. Considering how rapidly rain cell spatial structures evolve and how rain intensity varies with time, this close a time difference is essential in order to have a valid observation of the precipitation conditions affecting the QSCAT measurement. The 4 km resolution of NEXRAD is valuable for resolving the spatial variability.

A NEXRAD Level III "Composite Reflectivity" data product with 4 km spatial resolution, is shown in Figure (1). This depicts a maximum S-band reflectivity found on any constant elevation angle azimuthal sweep of a volume scan projected onto each Cartesian grid box [8]. The rainrate is displayed as a quantized color scale for the Reflectivity Factor, Z, in 5 dBZ steps. This example is from the Wilmington, NC station on Sept. 9, 1999. Buoy #41004 is indicated with a star symbol. The concentric circles are centered at the NEXRAD site (Lat. and Lon specified in figure), and represent

range steps of 115 km. The latitude and longitude grid lines are 1 degree each. Since the QuikSCAT resolution for a radar cross section cell is approximated to be a 28 km square, appreciable averaging of the NEXRAD 4 km resolution elements was necessary to create an equivalent spatial rain estimate. After converting the NEXRAD RCS from "dBZ" into rainrate and then averaging each 7-by-7 array (equivalent to a 28 km square area) a new data array of rainrate, centered at each QSCAT cell location, and compatible with the spatial resolution of satellite radar was produced. The buoy wind measurement, southeast of the rain area (location indicated by a star), was about 3 m/s for a two hour period centered at the time of the QSCAT overpass. Another buoy (# 41002) on the eastern side of this rain area (Lat. = 32.3°, Long.=75.4°) measured winds of about 5.5 m/s for a two-hour interval around the overpass time.

The locations of the QuikSCAT NRCS points used in this study were constrained to be no farther than 250 km from the NEXRAD station, over the ocean. Specifically, they lie between 32° and 34.5° latitude and -79.5° to -76° longitude. The reason is that the accuracy of near surface rain estimates decreases with distance from the NEXRAD. The NRCS data points were identified as either Horizontal or Vertical polarization and separated accordingly. This was straightforward since they have different incidence angles, 46° and 54° respectively. Another separation was made which selected NRCS points which were observed by the forward beam sweep of the satellite antenna. This effectively constrains all the data points to be within a narrow range of radar azimuth angles, when the area under study is much less than the 1400 km swath width. Each data point represents the average NRCS (σ_0) from an elliptically shaped cell 25-by-35 km. The center point of this cell is used as the center of a 28 km square area over which the mean rainrate is computed using the 4 km NEXRAD cells (from data shown in Fig. 1) formed into 7-by-7 arrays. Figure 2 shows the separate plots of V-pol and H-pol σ_0's (converted to decibels) versus the mean rainrates for each corresponding cell. Obviously, those NRCS cells which fall in an area without rainfall will not be plotted. The two data sets span a wide dynamic range; approximately 2 orders of magnitude. Even though these plots display considerable scatter for both quantities, there is a clear monotonic relationship between NRCS and rainrate. There is a fundamental distinction that contributes to the data scatter. The scatterometer operates effectively in a CW mode and integrates the rain backscatter throughout the full column in the line-of-sight. The size of the NRCS will depend on the height of the rain column and the rain profile within. The NEXRAD data product, measured in mm/hr, is more like a flux quantity representing a

flow rate at a specific reference height. In this case, it is the maximum value in a vertical column. Therefore variations in the length of the rain column will affect the NRCS but may not affect the NEXRAD product by the same amount. Another quantity that will cause scatter in the NRCS data is the variability of the drop size distribution. These uncertainties, while undesirable, does not appear to negate the usefulness of the relationship seen in this figure.

The lower graph of the H-pol data has been fit with a regression function to create a "Z-R" function for the Ku-band scatterometer. This function is similar to the one developed using a simple theoretical model for spherical raindrops [Weissman, et al, 2001]. This empirical function can then be used to estimate rainrates over the ocean, with cell sizes determined by the scatterometer resolution, once it has been determined that the scatterometer is receiving backscatter from rain volume. The prerequisite to applying this procedure is having a reliable "rain-flag"

At the wind speed regime which is believed to exist at the surface, if no rain were present, the NRCS data points for both polarizations would be in the range from -30 dB to -25 dB. For rainrates larger than 0.5 mm/hr the NRCS is found to equal or exceed these surface estimates, and both polarization σ_0's clearly increase proportionally to the rainrate. A more careful comparison of the data for rainrates larger than or equal to 1 mm/hr in Figure 3 shows that H-pol NRCS tends to exceed the V-pol. This effect, the differential reflectivity (Z_{DR}) is well known in the field of radar meteorology. The physical basis for this is the oblateness of raindrops, once they become larger than about 2 mm is diameter [9]. Fortunately, the normal no-rain relationship between the two polarizations is that V-pol exceeds H-pol by a few decibels or more, depending on the surface wind speed. Therefore, when an average surface area (say 0.25° Lat/Lon square) displays a higher NRCS for H-pol than V-pol, it is very likely that appreciable rain is present. This effect has been adopted as a "rain-flag". It is then used in conjunction with the Z-R formula derived from the H-pol data of Figure 2 to estimate rainrates in the open ocean. Note that while the swath of SeaWinds is 1600 km, the H-pol observations only cover a 1400 km swath.

IV. RESULTS

Several co-locations of the TRMM satellite and QuikSCAT were studied to determine the level of agreement between rain estimates produced by the passive microwave imager, TMI, and the method

discussed above. The TRMM product used here, which has a 760 km wide swath, contains daily files with 24 hourly segments of the orbit. The gridded rainrate estimates are in 0.5° cells in units of mm/hr, and are accompanied by the time of observation. The procedure used here is to survey the rain observations collected by TRMM and then seek a sufficiently close encounter (in space and time) with QSCAT. Numerous events have been studied with similar results.

A good example is an event of July 20, 2001 in an ocean region west of Nicaragua. A section of the hourly segment corresponding to 12:05Z is extracted from the TRMM data image (Figure 4). The features here are typical of many other observations. Relative small clusters of high rainrates, often exceeding 7 mm/hr, occur in areas of 1-to-2 degrees latitude and longitude. These are imbedded in much larger regions of lower rainrates.

A QuikSCAT orbit co-location was observed at 12:00Z, but with an oblique swath that covered only the region east of -99° longitude, and slanted to exclude some of the section below 8.5° latitude. The higher resolution of the QSCAT L2A data (the highest level data set containing backscatter observations) are used to estimate mean rainrates in 0.25° cells, using the Z-R relation discussed above. The rain rates are averaged again to create a matching 0.5° cell rainrate. Therefore, a sub-region of the rain seen by TMI (Figure 4) is plotted in Figure 5 (upper graph) for comparison with the new SeaWinds rain estimates in an identical region in the lower graph. The scatterometer rainrates (lower graph) are seen to provide a very similar spatial image of the rain occurrence and intensity. Some limitations are that the scatterometer may not detect some of the lower rainrates detected by TRMM, but this appears to be minor shortcoming. A point-by-point scatterplot of the TRMM versus QSCAT rainrates (Figure 6) shows those data points where neither has a zero value. The solid line indicates perfect agreement and the dashed lines show the limits for differences that are less than a factor of two. Clearly, most of the comparison points show that the QSCAT rain estimates are within a factor of two of the TRMM values. A simple summation of all TRMM and QSCAT rainrates over the entire region under study produces very close agreement (within 20%). This consistency will be useful if the two data sets are combined for monitoring precipitation over the global oceans. The general agreement between cell rainrates is better for those rainrates above 1 mm/hr. Possible reasons for disagreements at the lower rainrates are errors in either instrument at lower rainrates, variations in the height and uniformity of the rain column, and variations in the drop size distribution.

V. SUMMARY

This study provides evidence on the capability of SeaWinds scatterometer to estimate rainrates over the ocean. The relationships derived from empirical data are consistent with those used in radar meteorology, and applied to weather radar and the Tropical Rainfall Measurement Mission (TRMM). The principal algorithm was derived from collocated NEXRAD and QSCAT measurements. It also exploits the differential reflectivity associated with moderate and higher rainrates. Analysis is continuing to refine the features and quality of the algorithms for rain-flagging, and rainrate estimation (Z-R formula), in the future. Attention will also be directed at situations with strong wind, and storm conditions to test the usefulness and range of validity of this technique. Considering the wide swath of the scatterometer and its global spatial coverage, future applications for global precipitation studies are likely.

VI. ACKNOWLEDGMENT

This research was supported by the Physical Oceanography Program of the National Aeronautics and Space Administration through Grants to Hofstra University and the Center for Ocean-Atmospheric Prediction Studies, Florida State University (through support by NASA OVWST Project, the NASA/OSU SeaWinds Project and NOPP). We would also like to acknowledge the support provided by the National Weather Service through a COMET Partners Project Grant to Hofstra University administered by the University Corporation for Atmospheric Research, Boulder, CO. We are also grateful to Dr. James J. O'Brien of COAPS for his guidance and encouragement. The QuikSCAT Level 2A data was provided by the NASA Jet Propulsion Laboratory PO.DAAC

VII REFERENC

.M NAZ M.H. riel D G Lon "Spaceborn adar me urem
the an An ervi of th N CAT sc *Proc.* V N 0-: 66
99

M W C W D G Lo Imp ed re ol backsc te me its th
SeaW pe beam scatter te *EEE T G Re Sen* N 04
ary 2000

D W issm M A. Bo as an T gu "Effects n-rat an ma gn tud
W ds meter nd peed *A O Te* Vol N pp
May 002

C Ku al 000: "Th th trop fal mappi m (TRMM) af
orbi *App M* V N Dece be 000

R Mei T Ku *Spa boi W t'h Rada* 990 A H Bo ton MA. 99 pp

R Do ak. D an 93 *Doppler Radar and W O ms.* Edi
Academi Pr

A.R H me aff the po lar
to- G ge *Radi Sc* "(N 99 984

G Kl ira an D A. Imy A desc ial rod ab
NEXRAD W R D syst *A M ro Soc.* N pp

.N. B and V C dr kh *Dop W the iple nd*
App C U ty Pr 00 pp

FIGURE CAPTIONS

Figure 1. Composite reflectivity (quantized in 16 discrete levels of dBZ) derived from a six minute scan by the WSR-88D NEXRAD at Wilmington, NC on Sept. 9, 1999. Buoy # 41004 is indicated by a star symbol.

Figure 2. SeaWinds normalized radar cross section data (L2A files) vs. rainrate. Upper graph is V-pol data, lower graph is H-pol data. All azimuth look angles are in forward direction. Rainrate is determined from NEXRAD data shown in Fig. 1 (4 km resolution) averaged over a 28 km square areas centered at each SeaWinds cell. All NRCS data cells used were within 250 km limits from NEXRAD, shown in Fig. 1, and lay within a 150 km-by-150 km area. Winds: near buoy #41004 ≈3 m/s, at eastern edge, at buoy #41002, ≈5.5 m/s.

Figure 3. Combined plot of V-pol and H-pol data from Fig. 2, limited to rainrates greater than 1 mm/hr. The differential reflectivity between H-pol exceeding V-pol is apparent, notwithstanding the considerable scatter of each data set. A regression analysis of these two sets shows two different slopes for each polarization.

Figure 4. TRMM-TMI rainrate (0.5° Lat/Lon bins) measurements over ocean, west of Nicaragua, on July 20, 2001 at 12:00 GMT, within 5 minutes of a QuikSCAT overpass. The colorbar indicates rain intensity.

Figure 5. Comparison between SeaWinds rainrate estimates averaged over 0.5° to match TMI, the data of Fig. 4, which lie within the H-pol swath of the radar. Upper graph is the subset of the TMI measurements of Fig. 4; Lower graph are the SeaWinds rainrates estimates, derived from the H-pol data and a Z-R relationship derived from Fig. 2. The spatial pattern of rain detection by SeaWinds over this ocean region matches TMI very well. Note upper and lower colorbars are not identically calibrated.

Figure 6. Point-by-Point comparison of TMI rainrates versus SeaWinds rain estimates for cells shown in Fig. 5. The log-log plot was chosen for wide dynamic range. The solid line indicates perfect agreement, with the parallel dashed lines above and below indicating factor of two differences. A majority of data point comparisons lie within the dashed lines.

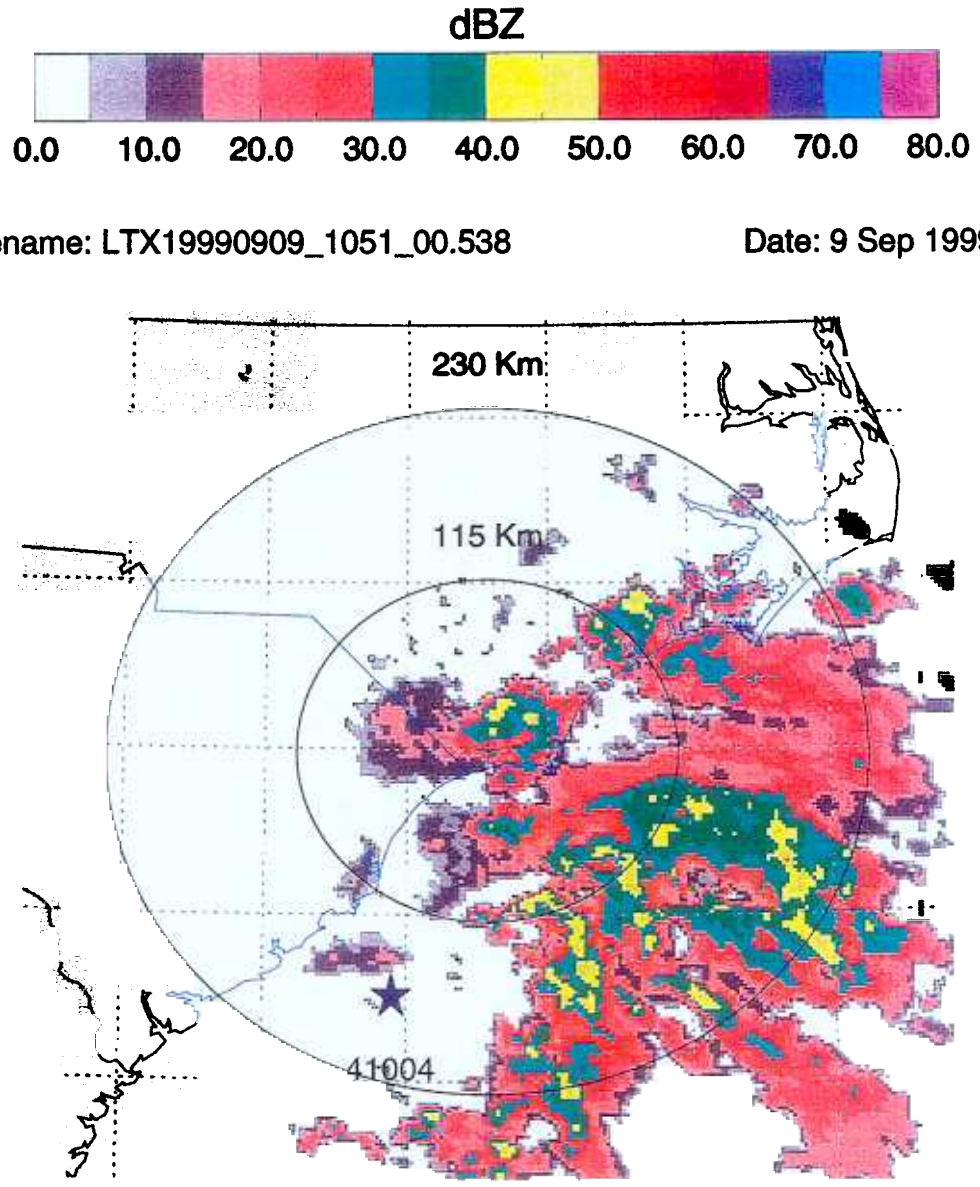
dBZ
0.0
10.0
20.0
30.0
40.0
50.0
60.0
70.0
80.0
Filename: LTX19990909_1051_00.538
Date: 9 Sep 1999
230 Km
115 Km
41004
Latitude: 33.59.20
Longitude: -78.25.44

Figure

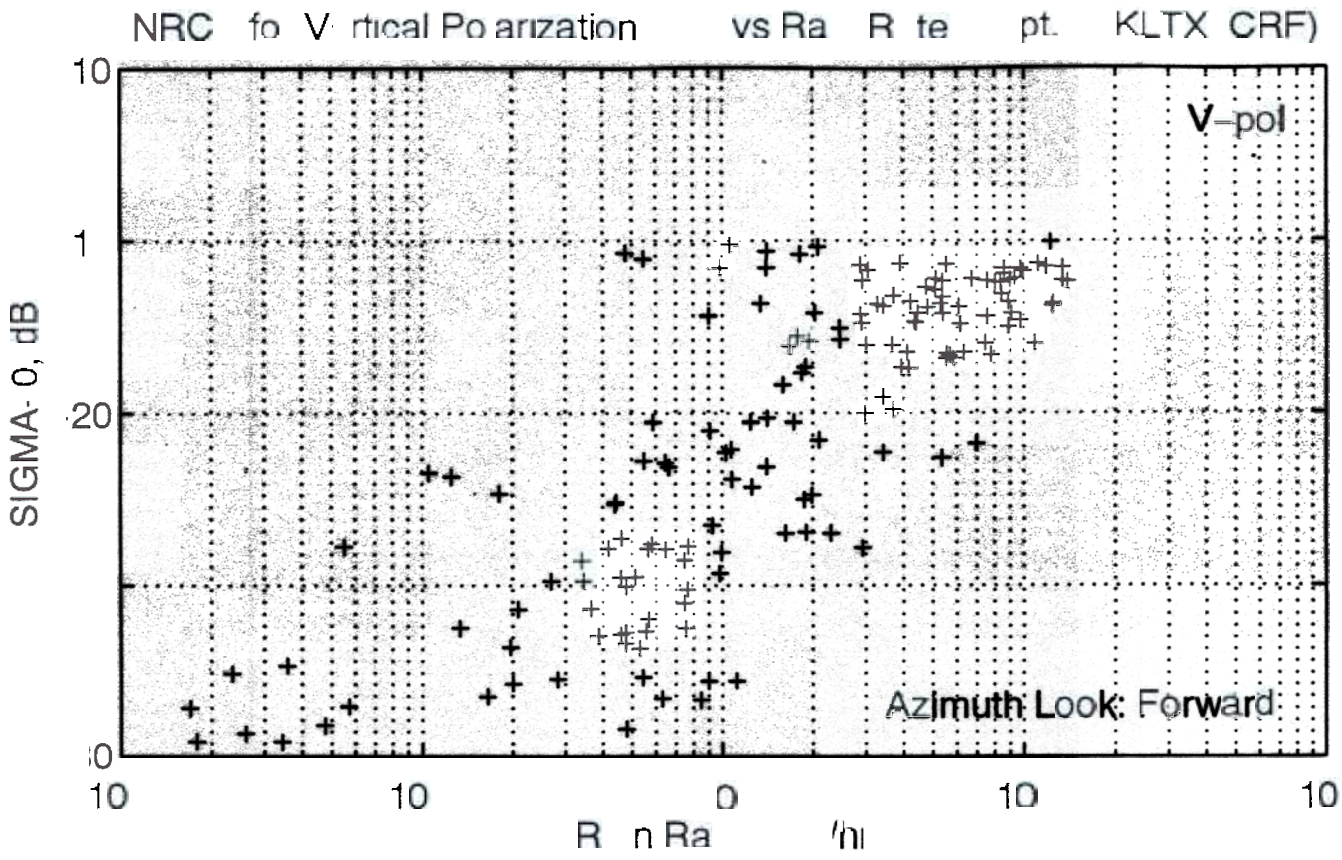
NRC fo V rtical Po arization vs Ra R te pt. KLTX CRF)
V–pol
Azimuth Look: Forward
SIGMA 0, dB
10
1
20
10
10
0
10
10
R n Ra /hr

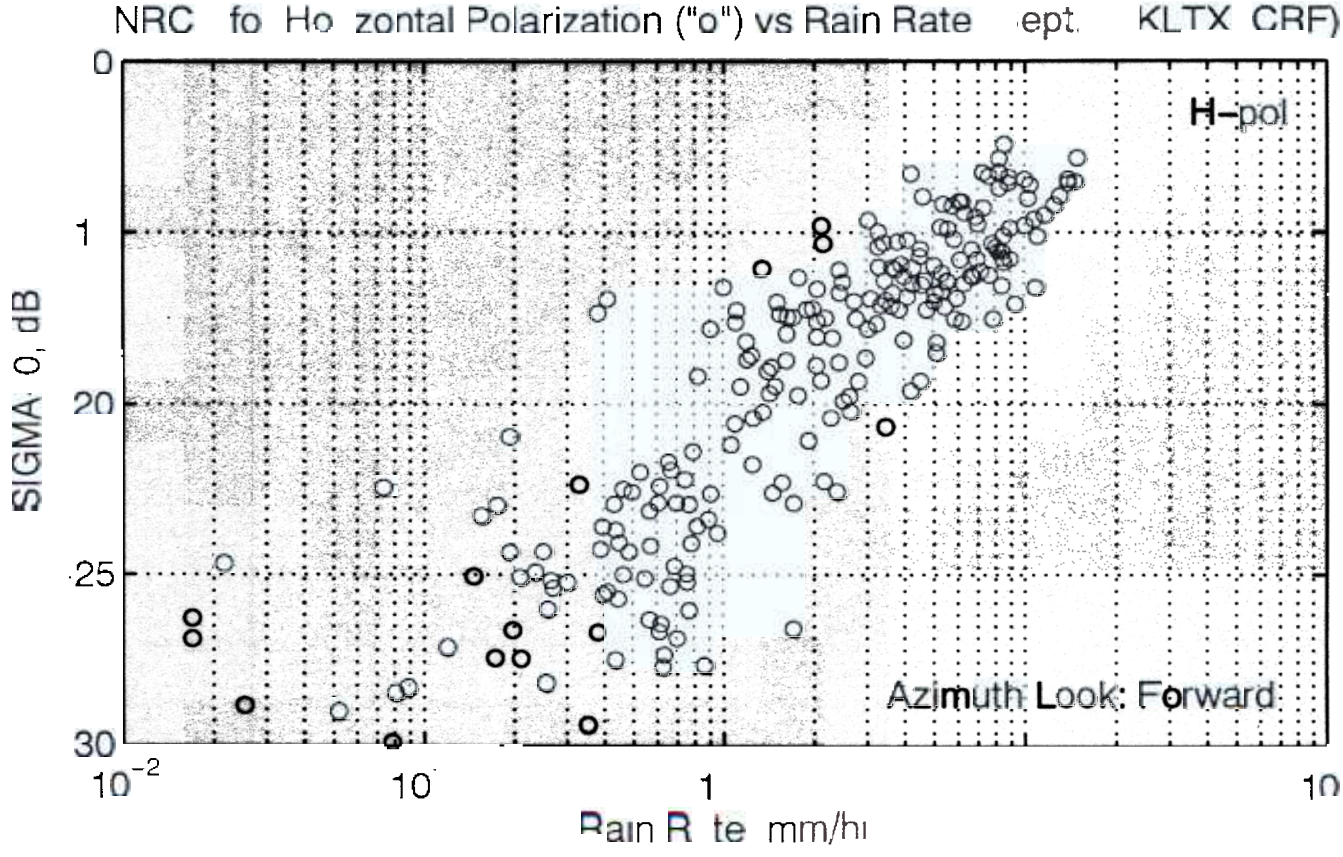
NRC fo Ho zontal Polarization ("o") vs Rain Rate ept. KLTX CRF)
H–pol
Azimuth Look: Forward
SIGMA 0, dB
0
1
20
25
30
10^-2
10
1
10
Rain R te mm/hr

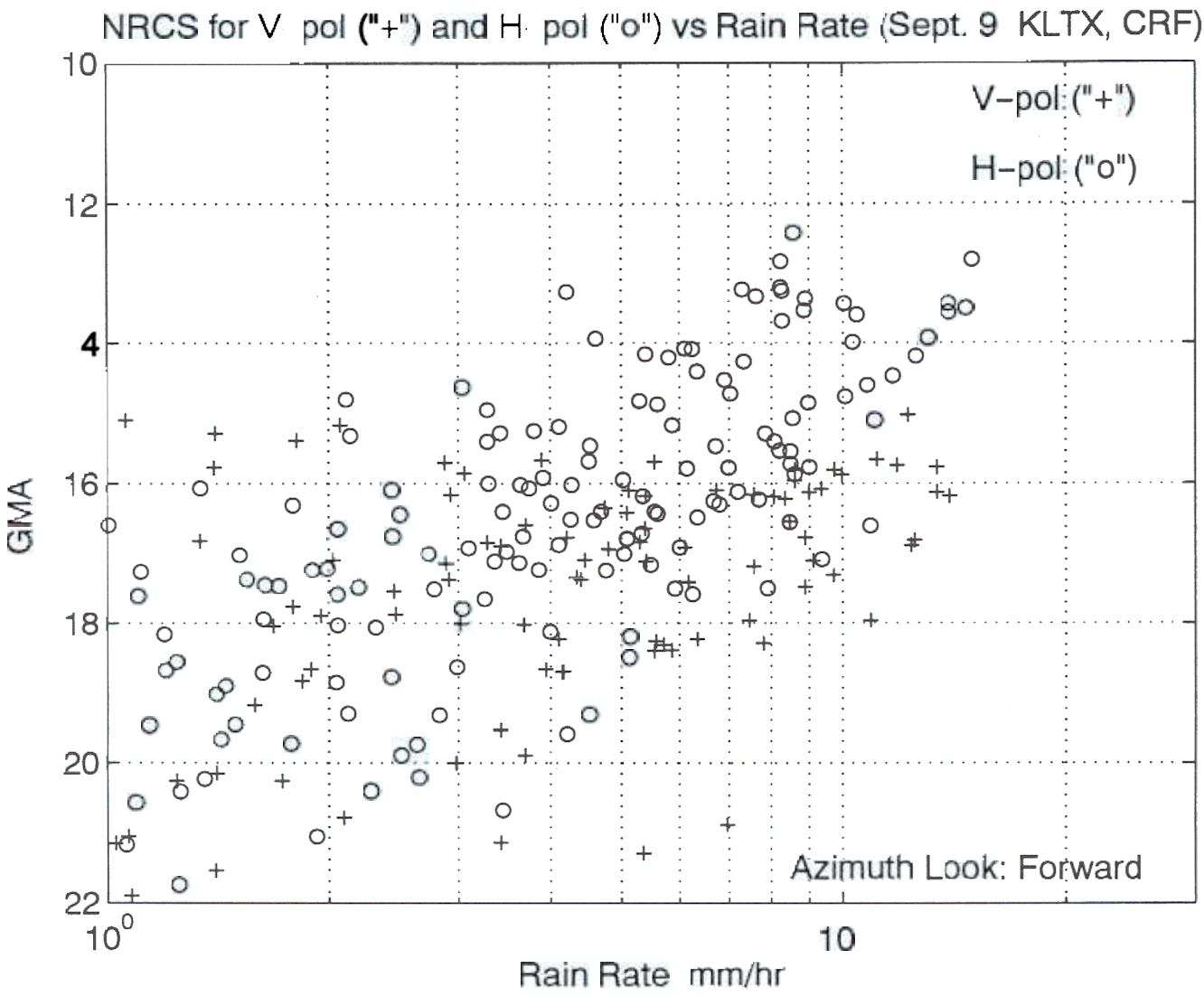
NRCS for V pol ("+") and H pol ("o") vs Rain Rate (Sept. 9 KLTX, CRF)
V-pol ("+")
H-pol ("o")
Azimuth Look: Forward
GMA
Rain Rate mm/hr
10
12
4
16
18
20
22
10^0
10

gure

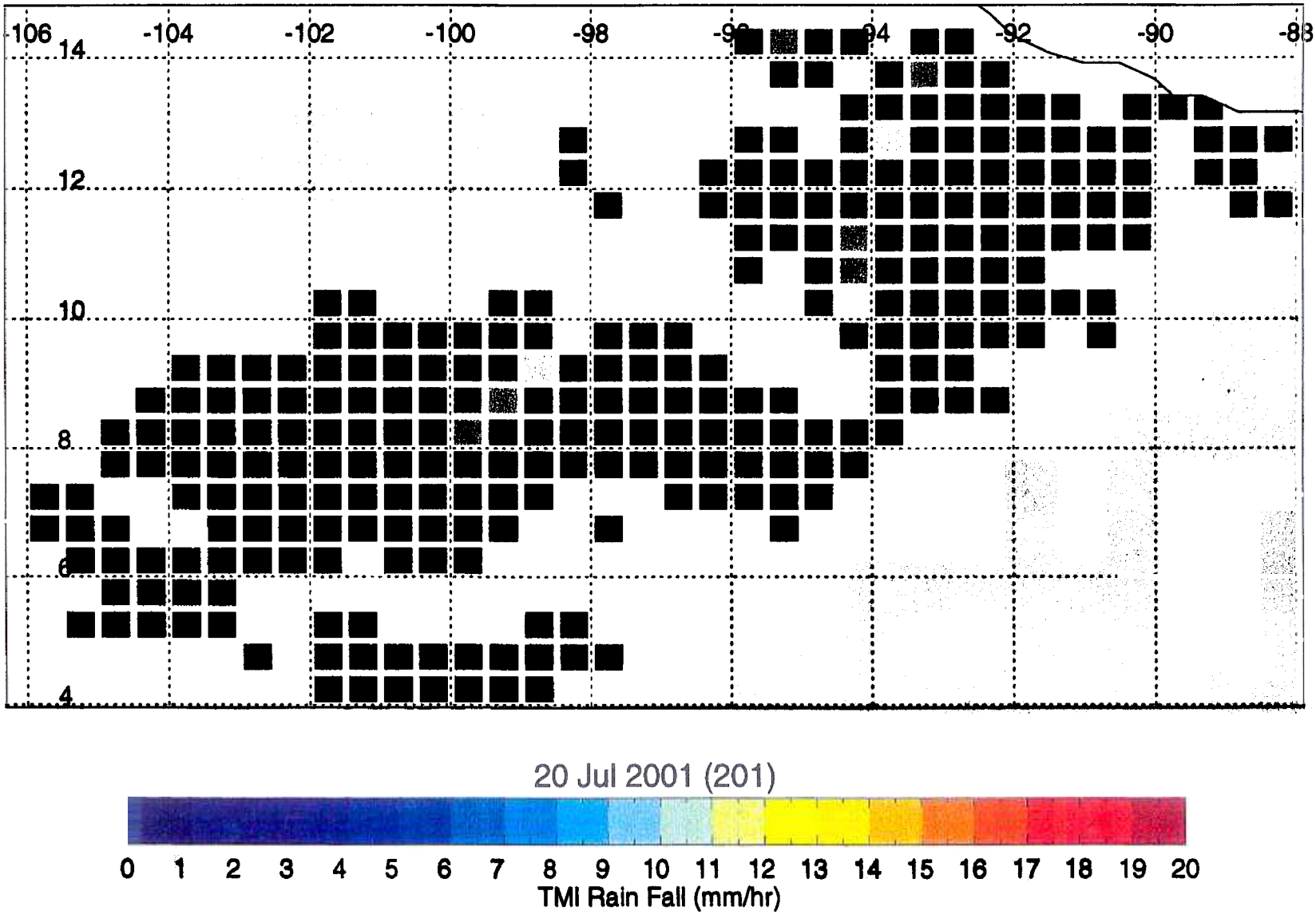
-106
-104
-102
-100
-98
-92
-90
14
12
10
8
6
4
20 Jul 2001 (201)
0 1 2 3 4 5 6 7 8 9 10 11 12 13 14 15 16 17 18 19 20
TMI Rain Fall (mm/hr)

Figure 4

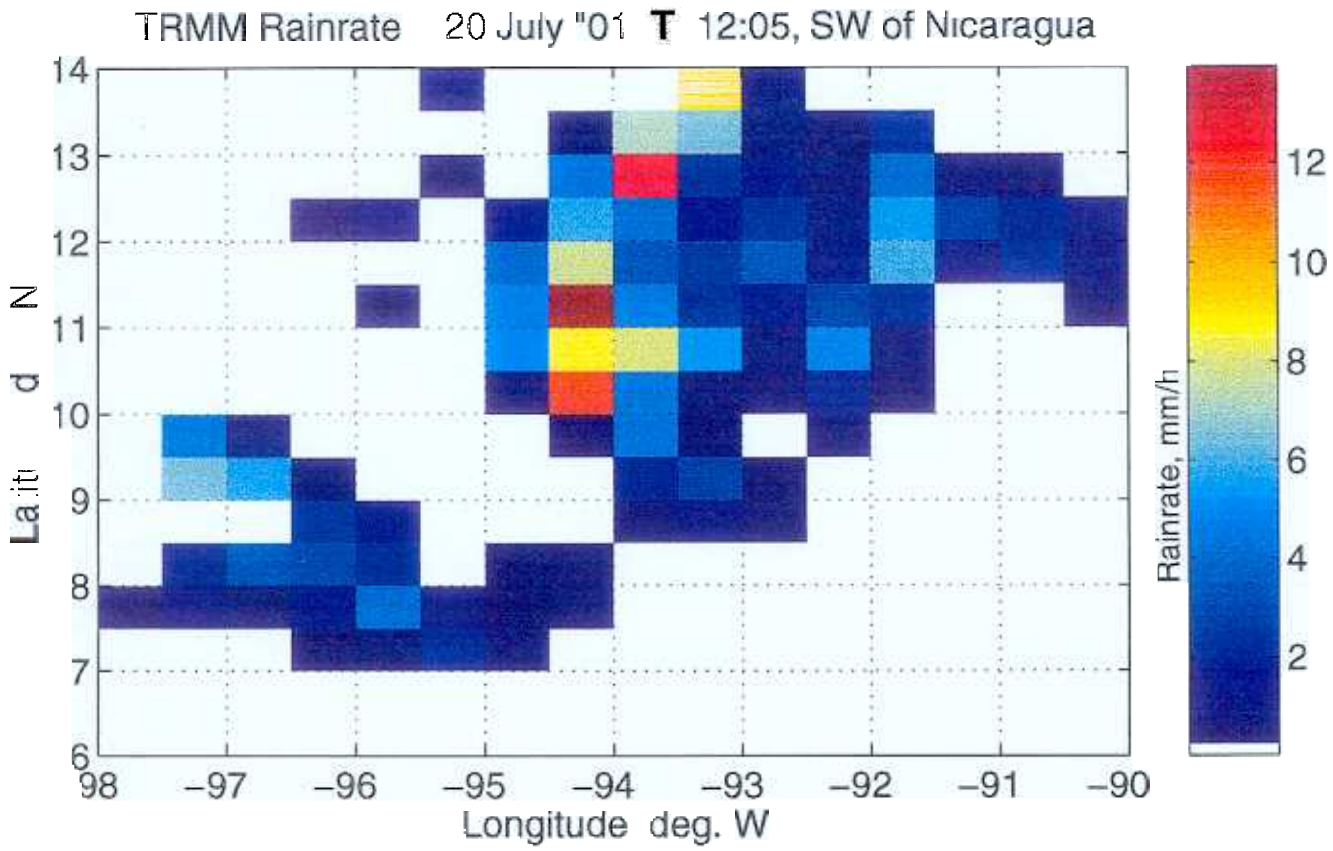
TRMM Rainrate 20 July "01 T 12:05, SW of Nicaragua
14
13
12
11
10
9
8
7
6
98 −97 −96 −95 −94 −93 −92 −91 −90
Longitude deg. W
Rainrate, mm/h
12
10
8
6
4
2

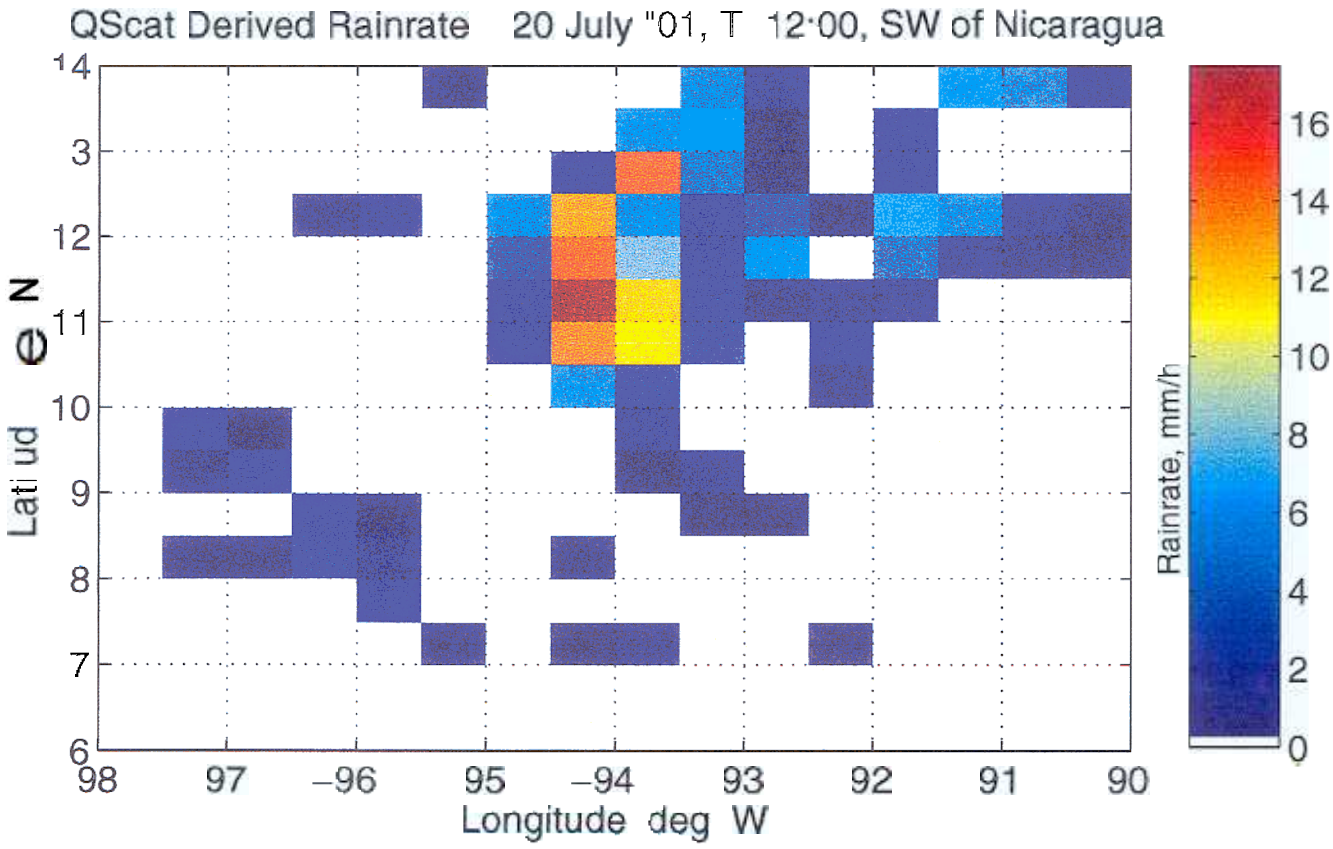
QScat Derived Rainrate 20 July "01, T 12:00, SW of Nicaragua
14
13
12
11
10
9
8
7
6
98 97 −96 95 −94 93 92 91 90
Longitude deg W
Rainrate, mm/h
16
14
12
10
8
6
4
2
0

gure

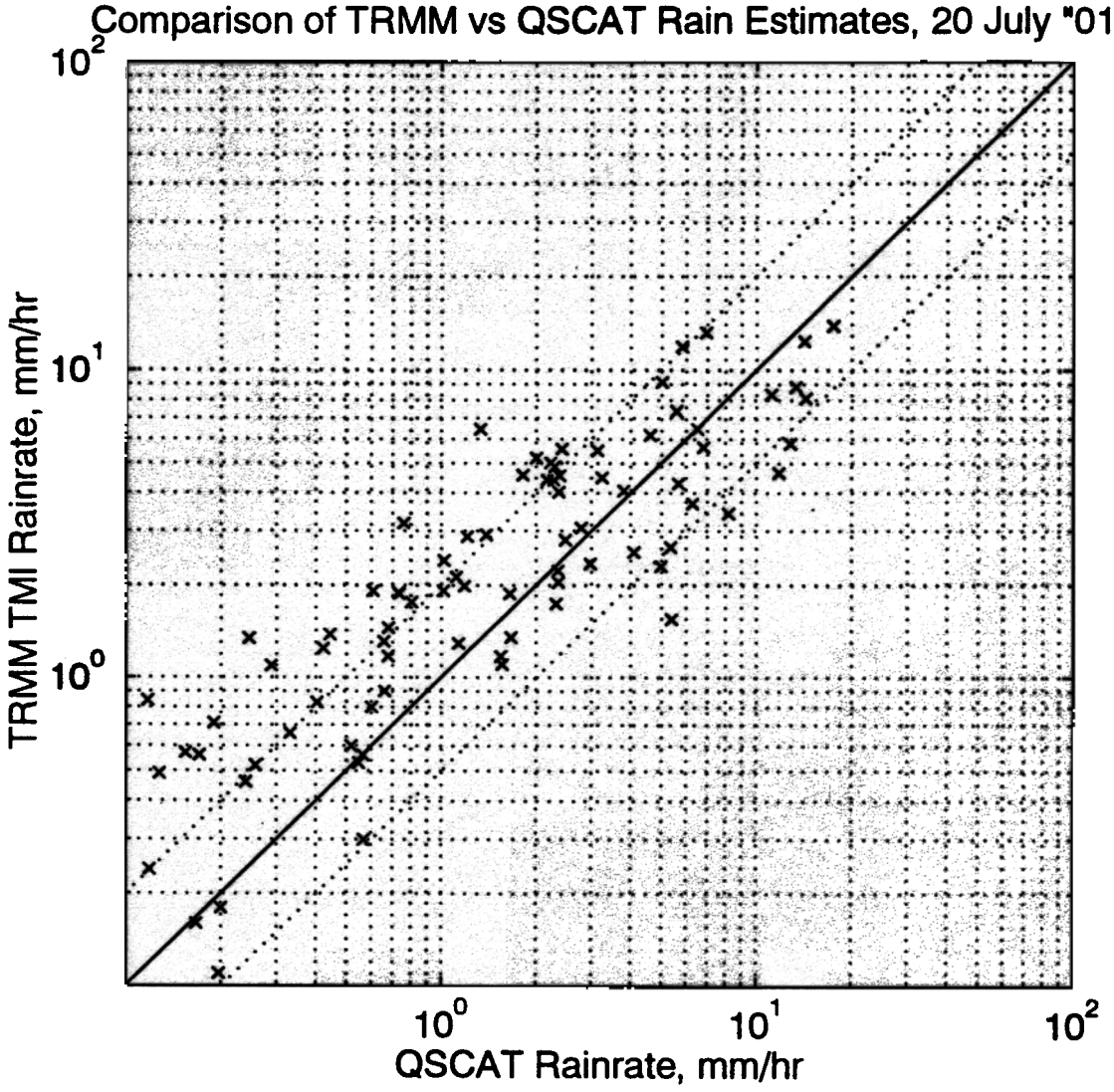
Comparison of TRMM vs QSCAT Rain Estimates, 20 July "01
TRMM TMI Rainrate, mm/hr
QSCAT Rainrate, mm/hr
10^2
10^1
10^0
10^0
10^1
10^2

Figure 6